Wireless Pers Commun
DOI 10.1007/s11277-011-0265-z

Intercell Interference Coordination Using Threshold-Based Region Decisions

Cheolwoo You · Gilsang Yoon · Changwoo Seo · Sherlie Portugal · Gihwan Park · Taejin Jung · Huaping Liu · Intae Hwang

Abstract IMT-Advanced mobile communication systems make it possible for any devices to access high-speed networks anytime and anywhere. To meet the needs of IMT-Advanced systems, cellular systems must solve the problem of intercell interference caused by frequency

"This work was supported by the 2011 research fund of Myongji University in Korea".
"This research was supported by the MKE (The Ministry of Knowledge Economy), Korea, under the ITRC (Information Technology Research Center) support program supervised by the NIPA (National IT Industry Promotion Agency) (NIPA-2010-C1090-1011-0008). This study was financially supported by Special Research Program of Chonnam National University, 2009. This work was supported by the National Research Foundation of Korea Grant funded by the Korean Government (NRF-2010-013-D00046)".

C. You
The Department of Information and Communications Engineering, Myongji University,
San 38-2 Nam-dong, Cheoin-gu, Yongin-si, Gyeonggi-do 449-728, Korea
e-mail: cwyou@mju.ac.kr

G. Yoon · C. Seo · S. Portugal · G. Park · T. Jung · I. Hwang (✉)
The Department of Electronics and Computer Engineering, Chonnam National University,
300 Yongbong-dong, Buk-gu, Gwangju 500-757, Korea
e-mail: hit@chonnam.ac.kr

G. Yoon
e-mail: luckyface0410@hanmail.net

C. Seo
e-mail: apples021@naver.com

S. Portugal
e-mail: supersher17@hotmail.com

G. Park
e-mail: parkpgh@naver.com

T. Jung
e-mail: tjjung@chonnam.ac.kr

H. Liu
The School of Electrical Engineering and Computer Science, Oregon State University,
Corvallis, OR 97331-3211, USA
e-mail: hliu@eecs.oregonstate.edu

Published online: 05 March 2011

reuse. Intercell interference problems become severe when orthogonal frequency division multiplexing (OFDM) transmission, which is a key technology for 4G communication systems, is used in a cellular system. In this paper, a zone-based intercell interference coordination (ICIC) scheme with high flexibility and low cost is proposed, and its performance is evaluated through multicell system-level simulations carried out according to the simplified 3GPP (3rd Generation Partnership Project) Long Term Evolution (LTE) system parameters. In the proposed algorithm, each cell is divided into several regions based on threshold values. Each region reuses frequencies in different ways, and the regions have different maximum transmit (TX) powers according to the interference environment. Even though the proposed scheme can be implemented with low complexity by using only the existing user equipment (UE) measurement, simulation results have confirmed that it provides significant improvements in geometry distribution.

Keywords IMT-Advanced · Intercell interference · ICIC · OFDM · LTE

1 Introduction

Mobile communication technology has been evolving to meet the needs of a communication market that demands high quality, high capacity, and high speed support. The goal of IMT-Advanced (i.e., 4G) mobile communication systems is for the remote unit to be connected to a network with data transmission speeds of 100 Mbps on the move and 1 Gbps when stationary [1–3]. Many techniques have been proposed and discussed to satisfy the requirements of 4G mobile communication systems.

Among these techniques, orthogonal frequency division multiplexing (OFDM) is a key technology. Because cellular systems try to achieve high-capacity and high-quality transmission within a given frequency range, they necessarily reuse the available frequency in each cell. Therefore, intercell interference is inescapable and must be solved, particularly for cellular systems using OFDM transmission, in which frequency reuse efficiency and performance of the user equipment (UE) at cell boundaries have deteriorated.

As a solution to these problems, various intercell interference mitigation techniques have been proposed. These techniques can be classified into three categories: Intercell interference randomization, intercell interference cancellation, and intercell interference coordination (ICIC). The main concept of interference randomization is to decrease collision probabilities by randomizing/whitening the interfering signal. Cell-specific interleaving and cell-specific scrambling are usually used for randomization [4]. Intercell interference cancellation is based on detection/subtraction of intercell interference. Some techniques spatially suppress interference by means of multiple antennas at the UE, beyond what can be achieved by just exploiting the processing gain. Sometimes interference randomization is combined with interference suppression or cancellation [5]. ICIC schemes aim to control interference through various methods such as frequency scheduling, modified frequency reuse, rotation of resource regions, power levels coupled to subband priorities, soft reuse, coordinated symbol repetition, and so on [6–21]. Because this kind of technique can be implemented using simple methods such as resource allocation, frequency-domain scheduling and power control, it has little effect on standards and thus is preferred by many researchers.

In this paper, a zone-based ICIC scheme with high flexibility and low implementation cost is proposed to increase average cell capacities through improvements on frequency reuse efficiency and to reduce outage probabilities for users on cell edges. We also propose a threshold-based region decision algorithm and a power control algorithm to increase the effectiveness of the proposed scheme. The proposed scheme divides an entire cell into several regions according to the interference environment. The frequency band is also divided into several subcarrier groups and the groups are assigned to the regions through frequency-domain scheduling. TX power is controlled differently for the regions.

The remainder of this paper is organized as follows. In Sect. 2, we explain representative conventional ICIC schemes and discuss several important characteristics that a good ICIC scheme is expected to have. In Sect. 3, we propose a zone-based ICIC scheme, and describe the basic parameters and definitions. Section 4 provides simulation results and comparisons obtained via system-level simulations, and this is followed by our concluding remarks in Sect. 5.

2 Conventional Schemes and Algorithm Development Strategy

2.1 Conventional ICIC Schemes

To increase cell-edge bit rate in the 3GPP LTE system, various ICIC schemes have been proposed to mitigate intercell interference [6–21]. From some points of view, the proposed schemes look very similar. The main idea is based on the principle of allocating “more bandwidth and less power” to inner cell users (ICUs) and “less bandwidth and more power” to cell-edge users (CEUs). For this purpose, the researchers consider a fractional reuse scheme in which part of the available resources is reserved for CEUs. In addition, they try to reduce intercell interference (i.e., improve a signal-to-interference plus noise ratio; SINR) at cell borders by dynamically or statically limiting the TX power on certain frequency bands.

A fractional frequency reuse (FFR) scheme to enhance the edge rate for the downlink (DL) of an OFDMA system was proposed in [6,7], where each cell reuses the frequency in different ways. This FFR scheme has reduced bandwidth overhead compared to traditional frequency reuse schemes. Unlike traditional reuse schemes, where the same frequency is only used in 1 out of 3, 7 or 12 cells, FFR gives UEs in different channel conditions to different frequency reuse patterns, that is, each UE is associated with a particular frequency reuse plan that corresponds to a frequency ‘reuse set’. The goal of FFR is to deploy frequency patterns such that a UE can avoid interfering with or being interfered by non-serving cells in its reuse set. Because cells in the reuse set are those that contribute most significantly to the overall interference on DL, avoiding interference from these cells is expected to effectively reduce the interference.

One exemplary FFR frequency plan with a maximum reuse set size of 3 is as follows: Define three over lapping frequency sets, F_1, F_2 and F_3. Only frequency tones that do not belong to the frequency set F_i, where $i \in \{1, 2, 3\}$, can be used for UEs served by *cell-i*. If a neighboring *cell-j* is added to the reuse set of a UE, the UE’s frequency tones are further restricted to $F_i^C \cap F_j$, as shown in Fig. 1.

A similar scheme to FFR was proposed in [8–10]. This scheme divides the whole band into multiple subbands, for example, 7 or 9, then each cell is assigned a subband to be used by the UEs close to the cell but belonging to neighbor cells. In this way, a UE close to a cell but not belonging to that cell is assigned a different subband from those used by the cell-edge UEs of that cell. A UE is allocated to a subband on the basis of which cell receives/transmits with highest power from/to it.

Another scheme based on FFR was proposed in [11–13], where diversity gain increases through rotation of resource regions. This scheme defines whispering and speaking regions, which are de-prioritized resource regions with lower transmission power and other regions,

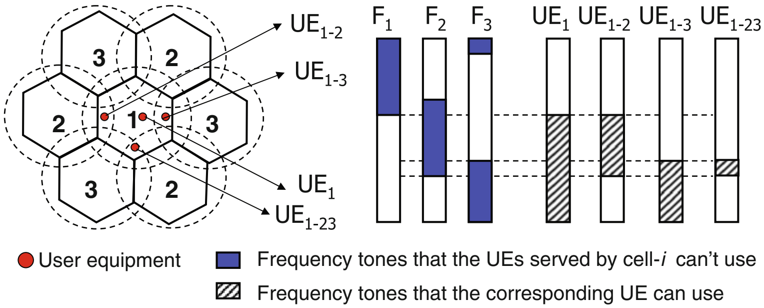

Fig. 1 One exemplary sector layout and reuse set assignment for the FFR scheme with maximum reuse set size 3

respectively. A UE using a whispering resource region is allocated a lower transmission power in DL and suffers higher intercell interference in uplink (UL). On the contrary, UEs using speaking resource regions on cell boundaries achieve higher performance.

A soft frequency reuse (SFR) scheme, in which each cell reuses a subdividable frequency through resource power control, was proposed in [14,15]. SFR is characterized by a frequency reuse factor of 1 in the central region of a cell, and by a frequency reuse factor greater than 1 in regions close to the cell edge. This scheme divides the whole band into two subcarrier groups, major and minor. Major subcarrier groups between neighbor cells are orthogonal, and can therefore be used by all the UEs in a cell. A minor subcarrier group cannot be used by cell-edge UEs, therefore minor subcarrier groups do not need to be planned between neighbor cells. A UE is allocated to each subcarrier group based on its power.

Another SFR scheme divides the whole band into two subcarrier groups, that is, one subcarrier group to be used by CEUs and the other to be used by all the UEs in a cell [4,16]. The subcarrier group used by CEUs should be planned orthogonally between neighbor cells. One example given in [4] divides the whole band into three subbands and one of which is allocated to a subcarrier group used by CEUs.

Another kind of ICIC method is a partial frequency reuse (PFR) scheme. The PFR proposed in [17,18] divides the whole band by N subbands, so that X subbands are used by CEUs and $N - X$ subbands are used by the other UEs. Therefore, the subbands used by CEUs should be planned orthogonally between neighbor cells. The frequency reuse factor can be adjusted by adjusting the number X. A UE is allocated to a subcarrier group on the basis of its geometry, i.e., the ratio of intercell power and intracell power.

On the other hand, the ICIC scheme proposed in [19] divides the whole band into multiple subbands, then each subband of a cell is assigned a resource allocation priority and subbands with higher priority are allocated to higher TX power UEs. Resource allocation priority of the subbands should be defined to minimize overlap of high power transmissions between neighbor cells. It is possible to assign an equal resource priority to more than one subband. In [20], neighbor cells apply the same rule of UL TX power allocation within the frequency band, that is, UEs are allocated to frequency bands in order of path loss or target signal to noise ratio (SNR).

2.2 Algorithm Development Strategy

Through consideration of the aforementioned ICIC schemes, we can see several important characteristics to consider when developing an excellent ICIC scheme. Because ICUs usually have sufficient power, the main constraint on performance improvement is available bandwidth. Therefore, it is best to assign the maximum possible bandwidth to ICUs, for example, the whole bandwidth. In contrast, due to severe interference, the main constraint on CEUs is bad SINR, and the expansion of available bandwidth will not improve performance. Therefore, it is important to decrease intercell interference at cell boundaries. This can be achieved by fractional frequency reuse, an interference cancellation technique, or a combination of both.

We think that region-based resource allocation is one of the most effective methods to differentiate CEUs and ICUs and cope with their distinctive features. If region-based resource allocation borrows the concept of fractional/soft/partial frequency reuse, it can reduce higher cochannel interference (CCI) levels incurred at cell boundaries as well as use resources efficiently. For example, parts of frequency bands are reserved for CEUs in order to reduce interference experienced by these UEs. This kind of ICIC scheme (i.e., region-based resource allocation combined with a modified frequency reuse concept such as FFR, SFR, PFR, and so on) can be operated by Node-B DL scheduling, and thus it may have no impact on standard specifications and can be easily and practically implemented. Of course, the amount of information to be shared by adjacent cells in order to operate a region-based ICIC scheme has to be reasonable.

On the other hand, to guarantee the effectiveness of a region-based ICIC scheme, a systematic method for region decisions should be developed. In addition, if maximum TX power can be controlled differently for regions according to their interference situations, such as allocating more power to weak users to guarantee reliable transmission, the region-based ICIC scheme will be more effective.

In the next section, we describe our proposal, designed by appropriately integrating the aforementioned characteristics.

3 Intercell Interference Coordination Using Threshold-Based Region Decision

3.1 Basic Parameters and Definitions

Here we explain the basic parameters and definitions for the proposed ICIC scheme. First of all, we define the frequency bandwidth set (FBS) $\{B(1), B(2), \ldots B(N_{max})\}$, where N_{max} is a positive integer and $B(i)$ is the frequency band assigned to the i-th enhanced node B (eNB) for a particular purpose, such as preferred or reluctant (un-preferred) bandwidth for some users. $B(i)$ can be defined by the i-th eNB, based on some gathered information such as the channel quality feedback by UEs. Because cells are probably connected to one another via the $X2$ interface in the 3GPP LTE system [22,23], adjacent cells can share FBS information through coordinated networking. If a central eNB is implemented [24–26], the value of $B(i)$ can be defined by the central eNB to which the i-th eNB belongs. In this case, the central eNB reports the FBS information to related cells via $X3$ interface and can effectively control intercell interference in a centralized manner. Of course, $B(i)$ can be changed (non-)periodically according to the interference environment.

The bandwidth size of $B(i)$ is defined by $BW(i)$, expressed by the unit, FBW_B. If we want to apply the proposed algorithm to the 3GPP LTE system, we only need to set $FBW_B = \triangle f \times N_{SC}^{RB}$, where N_{SC}^{RB} is the resource block size in the frequency domain, expressed as a number of subcarriers as defined in the 3GPP LTE standard [27].

SB_i and EB_i indicate the starting and ending points of $B(i)$, respectively, and they satisfy the following equation for the definition of the 3GPP LTE standrd:

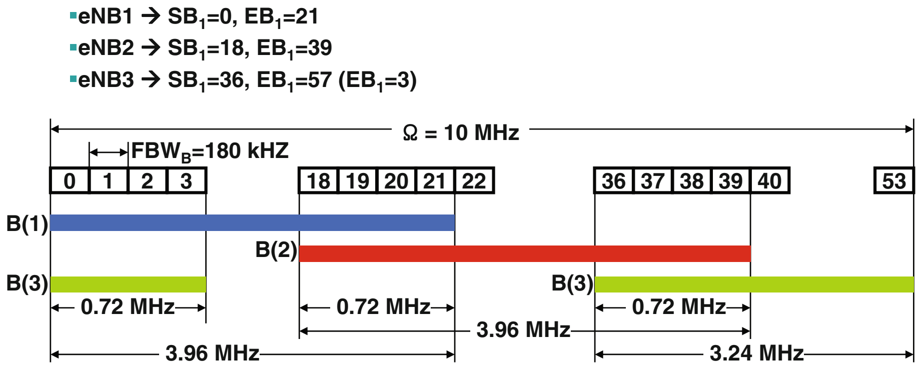

Fig. 2 The example of bandwidth allocation

$$N_{RB}^{min,DL} - 1 \le SB_i \quad \text{or} \quad EB_i \le N_{RB}^{max,DL} - 1, \tag{1}$$

where $N_{RB}^{min,DL} - 1$ and $N_{RB}^{max,DL}$ are the smallest and largest DL bandwidth configurations, expressed in multiples of N_{SC}^{RB}, respectively. In Eq. (1), if SB_i or EB_i is greater than $N_{RB}^{max,DL}$,

$$SB_i \quad \text{or} \quad EB_i = (SB_i \quad \text{or} \quad EB_i) \quad mod \quad (N_{RB}^{max,DL}). \tag{2}$$

Therefore, if $SB_i > EB_i$, the assigned bandwidth consists of frequencies indicated by $\{SB_i, \ldots, N_{RB}^{max,DL} - 1\}$ and $\{0, \ldots, EB_i\}$. For example, if $\triangle f = 15$ kHz and $N_{SC}^{RB} = 12$, then FBW_B is 180 kHz and $N_{RB}^{max,DL} = 54$ for a 10 MHz bandwidth.

Figure 2 shows the example of bandwidth allocation when the given constraints are $B(i) \cap B(j) \neq \{\ \}$ and $B(1) \cap B(2) \cap B(3) = \{\ \}$, i.e., no region with reuse 1. In this paper, we assume that all cells have the same available entire bandwidth, equal to Ω. Note that FBS is a logically defined frequency band and thus can be implemented using physical channels consisting of localized or distributed frequencies.

In this paper, geometry is used to analyze results and evaluate performance. In general, a geometry estimate for universal reuse can be expressed as

$$G = \frac{C_{serving}}{N + \sum C_{non-serving}}, \tag{3}$$

where $C_{serving}$ and $C_{non-serving}$ are the pilot strengths of a serving cell and any acquired non-serving cell, respectively, and N is the noise power, which includes both thermal noise and pilot interference from cells not acquired by the UE [6]. In future wireless cellular communication systems, we can assume that an advanced multiple access scheme or receiver will be used. Thus, the intracell interference can be eliminated. In this case, the geometry of a reuse set in cellular systems using the FFR concept for interference mitigation can be calculated by [14]

$$G = \frac{P_{rx}}{P_{inter-cell} + \frac{P_n}{R}}, \tag{4}$$

where P_{rx} is the received power of the expected user signal, $P_{inter-cell}$ is other cell interference power, P_n is white noise power, and R is the frequency reuse factor defined by

$$R = \frac{Total\ bandwidth}{Reused\ bandwidth}. \tag{5}$$

3.2 Proposed ICIC scheme

Here we propose a zone-based ICIC scheme with high flexibility and low implementation cost, aimed at achieving effective spectrum use as well as mitigating interference. For convenience of explanation and illustration, in this paper we assume that each cell uses one of the three reuse patterns and $B(i) \in \{B(1), B(2), B(3)\}$ for all i, without loss of generality. In this case, $ICU(i)$ and $CEU(i)$ indicate inner cell users and cell-edge users served by the eNB using $B(i)$ for $i = 1, 2, 3$, respectively. In addition, a hexagonal omni-cellular structure is assumed, because it is equivalent to a hexagonal three sectored multi-cellular environment, i.e., omni-cells can be directly applied to sectored-cells [11].

The proposed ICIC algorithm can be summarized as follows:

- In each cell, the available total subcarriers are logically divided into two bands. That is, $\Omega = B(i) \cup B(i)^C$ for the i-th eNB. $B(k)$ is the reluctant bandwidth for $CEU(k)$. Basically, $B(k)$ can not be used by $CEU(k)$. However, $B(k)$ can be partially used by $CEU(k)$ under special conditions.
- $ICU(k)$ can freely use Ω, and thus can achieve an extremely high data rate.
- When $CEU(k)$ is interfered with by the cell using $B(j)$ for $j \neq k$ to a considerable extent, $CEU(k)$ should use some portion of $B(j)$ in principle. However, $CEU(k)$ can use all the parts of $B(j)$ under special conditions.

In the proposed algorithm, some portion of $B(k)$ is an optional usable frequency band. Naturally, by adding this optional usable frequency band, interference will increase because the band can be used simultaneously by several users. Therefore, a user who wants to use this frequency band needs an interference cancellation technique. If the user has no interference canceller or does not want to use it, the optional usable frequency band can be used only after sending a Monopoly Indication (MI) to the corresponding interfering cell(s) through the $X2$ interface, to indicate the intention to exclusively use the optional usable frequency band, and it can be implemented with just one bit (i.e., on/off indication).

Figure 3 shows one example of possible implementations of the proposed ICIC algorithm. The parameters shown in this figure are defined by

$$U_{i,ICU} = \Omega, \tag{6}$$
$$U_{i\to j,CEU} = B(i)^C \cap B(j), \tag{7}$$
$$U_{i\to jk,CEU} = B(i)^C \cap B(j) \cap B(k), \tag{8}$$
$$C_{i\to j,CEU} = B(i) \cap B(j), \tag{9}$$
$$C_{i\to jk,CEU} = B(i) \cap B(j) \cap B(k). \tag{10}$$

In Eqs. (6)–(8), $U_{i,ICU}$, $U_{i\to j,CEU}$, and $U_{i\to jk,CEU}$ indicate the frequency tones that can be used freely by $ICU(i)$, $CEU(i)$ interfered by $B(j)$ for $i \neq j$, and $CEU(i)$ interfered by $B(j)$ and $B(k)$ for $i \neq j$ and $i \neq k$, respectively. In comparison, the frequency tones given by Eqs. (9) and (10) can be used only conditionally by $CEU(i)$ interfered by $B(j)$ and $CEU(i)$ interfered by $B(j)$ and $B(k)$, respectively.

As shown in Fig. 3, we can classify whole frequency tones into three classes: BW_U, BW_{C1} and BW_{C2}, where BW_U is the freely usable frequency band, and BW_{C1} and BW_{C2} are the optional usable frequency bands. Note that if $CEU(i)$ uses BW_{C1} without an MI, the user can be interfered with mainly by one other user at most. When using BW_{C2} without an MI, $CEU(i)$ can be interfered with mainly by two users at most. Of course, when using an MI, $CEU(i)$ can use BW_{C1} and BW_{C2} with no interference.

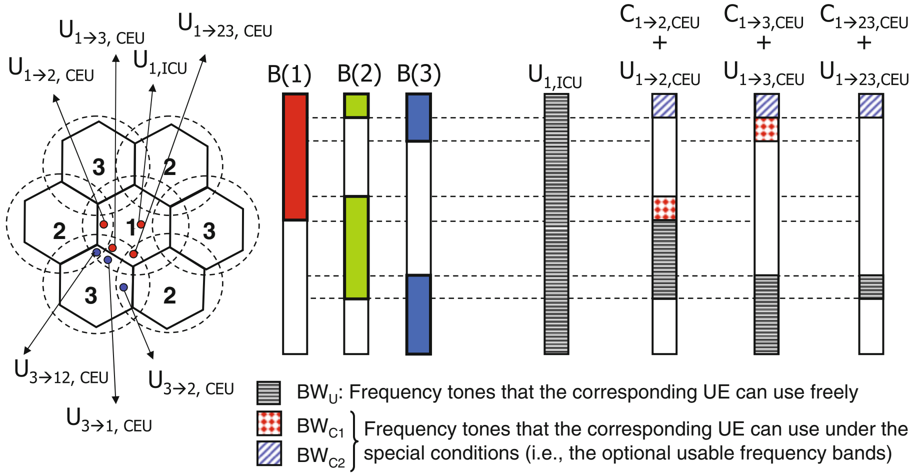

Fig. 3 One example for illustrating the frequency reuse concept of the proposed ICIC algorithm

On the other hand, if $B(1) \cap B(2) \cap B(3) = \{\quad\}$, the optional usable frequency bands are interfered with mainly by one user at most.

3.3 Threshold-Based Region Decision

In this subsection, a simple method of defining regions using the existing measurements of conventional systems, which we call threshold-based region decisions (TBRD), is proposed. The region in which the UE is located is specified by the TBRD, which uses thresholds and UE measurements. Then, the zone-based allocated resources defined by the proposed ICIC algorithm are assigned to UEs in the pertinent region.

Figure 4 is a flowchart illustrating one example of practical implementation of the TBRD, where t is the operation time unit for the region decision. In this figure, regions are classified into four decision categories using two thresholds and two UE measurements. The first threshold, *Thr1*, defines the boundary between the inner and outer (i.e., cell-edge) regions of the serving cell. The second threshold, *Thr2*, defines the motion direction of the UE.

The UE measurements are the reference signal received power (RSRP) and the interference over thermal (IoT), which are being already measured by UEs in conventional systems [28]. In TBRD, UE measurements are filtered to prevent too frequent region changes. The filtered UE measurements on an arbitrary Cell-r are defined by

$$M1(r) = Filter1(RSRP\_r), \tag{11}$$
$$M2(r) = Filter2(IoT\_r), \tag{12}$$

where RSRP_r and IoT_r are the measured values based on signals transmitted from Cell-r, and $Filter1(\cdot)$ and $Filter2(\cdot)$ are some arbitrary functions that can be implemented by FIR or IIR filters.

On the other hand, the decision categories are given in Table 1, where it is assumed that Cell-i is the serving cell, and Cell-j and Cell-k are the interfering cells.

Note that the distribution of each region and the amount of intercell interference can be efficiently managed through changes in the threshold values, decision categories, the time constant of filter, the decision procedure, and so on. Therefore, we can actively control the

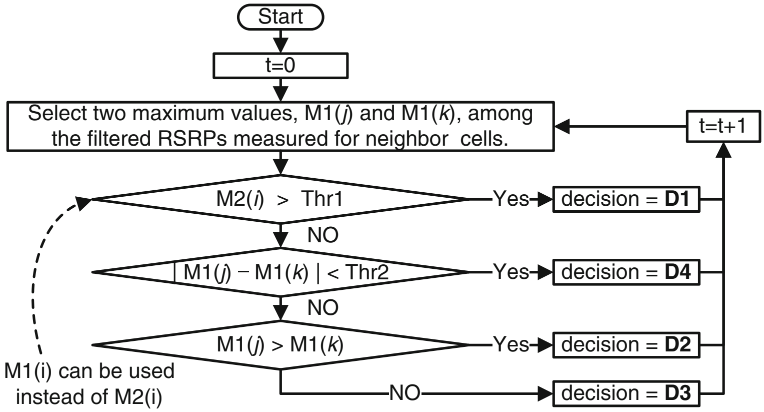

Fig. 4 One example of practical implementation of the proposed TBRD, where Cell-i is assumed to be the serving cell

Table 1 Definition of decision categories

Decision	Definition
$D1$	Inner region of the serving cell (No or low interference region)
$D2$	UE is moving from Cell-i to Cell-j (The region interfered with by one cell)
$D3$	UE is moving from Cell-i to Cell-k (The region interfered with by one cell)
$D4$	UE is moving from Cell-i to Cell-j and Cell-k (The region interfered with by two cells)

trade-off between the outage probability of cell-edge users and the frequency reuse efficiency (i.e., the average cell capacity).

3.4 Zone-Based Restriction on Maximum TX Power

As mentioned earlier, TX power control in combination with ICIC algorithms is very effective. To achieve this, first we classify interference zones into three types: interference-free zone (IFZ), low-interference zone (LIZ), and interference zone (IZ). LIZ means there is no need to do something extra to mitigate interference. IZ is divided into two types according to the ability to cancel interference: interference cancellation zone (ICZ) and high-interference zone (HIZ). We impose a limit on the maximum TX power according to the interference zones, i.e., zone-based restriction on maximum TX power (ZBRMTP). Table 2 shows one example of zone classification according to the interference situation. In this case, it is quite reasonable to determine maximum TX power levels as follows:

$$IFZ \geq ICZ \geq LIZ \geq HIZ. \tag{13}$$

For practical applications, we can use the indicator on an event-triggered basis, with the event being TX power exceeding a certain limit given by ZBRMTP. This is based on maximum TX power relative to the rated output power currently allocated by eNB or central eNB.

Table 2 Example of zone classification according to interference situation

Whether CEUs in neighbor cells can use the frequency tones or not	Inner region of serving cell	Outer region of serving cell
No	IFZ or LIZ	IZ (ICZ or HIZ)
Yes	IFZ	IFZ or LIZ

Frequency granularity can be the physical resource block (PRB) defined in [27,29]. In this case, a proactive indicator of relative and narrowband TX power with one bit per PRB can be exchanged among neighbor eNBs to support DL ICIC and DL scheduling. A bitmap can be used for several PRBs.

4 Simulation Results

We next describe the performance of the proposed scheme obtained by system-level simulations. In order to investigate the performance of the proposed algorithm, first we observed the cumulative distribution function (CDF) of user geometry, and then measured the average cell capacity and the 5% cell edge capacity as performance metrics. The 5% cell edge capacity indicates the average capacity of the lowest 5% users in geometry, who are practically located at cell edges with poor receiving environments. Thus, the 5% cell edge capacity is suitable for analyzing the effect of interference mitigation.

In addition, performance was evaluated in comparison with the conventional scheme proposed in [11,13], which effectively improves cell-edge performance, but slightly reduces the average data rate when compared to systems with no interference mitigation or only interference avoidance.

In every system-level simulation run, we consider the DL of a three-tier multi-cell wireless system with 19 cells, where it is assumed that each cell/site has one sector, because we have explained that a hexagonal omni-cellular structure is equivalent to a hexagonal three-sectored multi-cellular environment. The simulations were carried out on the 3GPP LTE system [30]. Detailed parameters are given in Table 3, where the inter-site distance (ISD) is set to 500 m to simulate an interference-limited micro-cell.

Table 4 shows the resource allocations of the proposed and conventional schemes for the simulations. In the conventional scheme of Table 4b, $W_{i,ICU}$ and $S_{i\rightarrow j,CEU}$ indicate the frequency tones that are used by $ICU(i)$ and $CEU(i)$ interfered with mainly by $B(j)$, respectively. IC indicates the frequency tones that are used simultaneously by all neighboring CEUs and for which interference cancellation should be used. In this case, low TX power is used for $W_{i,ICU}$, but high TX power is used for $S_{i\rightarrow j,CEU}$ and IC.

For convenience of comparison and implementation, we assume that the two schemes use only two values for maximum TX power, i.e., *TxPwrLow* and *TxPwrHigh*. In the proposed scheme, $ICU(i)$ uses *TxPwrLow*, but $CEU(i)$ uses *TxPwrHigh* or *TxPwrLow* when using resources of $B(i)^C$ or $B(i)$, respectively. In the conventional scheme, *TxPwrLow* is used for $W_{i,ICU}$, but *TxPwrHigh* is used for $S_{i\rightarrow j,CEU}$ and IC.

Note that the proposed scheme does not use the MI, for the sake of fairness.

First we observed the cumulative distribution function (CDF) of user geometry. Figure 5 shows the CDF of geometry according to *Thr1* when the proposed ICIC scheme uses *Thr2* $= 0$ dB and $PWR\_r = 0.1$, where

Table 3 Parameters for system-level simulation

Parameter	Value
Cell structure	Hexagonal grid, 3-tier, 19 cells, 1 sector/site
Antenna (Ant.) config.	BS: 1 , MS: 1
PRB	Freq. BW = 900 kHz, Time Dur. = 1 ms
BS Max TX power	46 dBm − 10 MHz carrier
Center frequency	2.0 GHz
Bandwidth	10.8 MHz
Cell radius = ISD/$\sqrt{3}$	500/$\sqrt{3}$ =∼ 289 m
Path loss model	$128.1 + 37.6 log10(R)$, R in km
Shadow std. deviation	8 dB
Penetration loss	20 dB
Thermal noise density	174 dBm/Hz
UE noise figure	9 dB (UE), 5 dB (eNB)
Corr. dist. of shadowing	50 m
Dist. betw. UE and eNB	>= 35 m
BS ant. gain	6 dBi with omni-antennas with cable losses
Ant. pattern	Omni-directional

Table 4 Resource allocations for system-level simulation

(a) The proposed scheme

<table>
<tr><th>PRB</th><th>Cell-1</th><th>Cell-2</th><th>Cell-3</th></tr>
<tr><td>0</td><td rowspan="6">B(1)</td><td rowspan="4"></td><td rowspan="2">B(3)</td></tr>
<tr><td>1</td></tr>
<tr><td>2</td><td rowspan="6"></td></tr>
<tr><td>3</td></tr>
<tr><td>4</td><td rowspan="6">B(2)</td></tr>
<tr><td>5</td></tr>
<tr><td>6</td><td rowspan="6"></td></tr>
<tr><td>7</td></tr>
<tr><td>8</td><td rowspan="4">B(3)</td></tr>
<tr><td>9</td></tr>
<tr><td>10</td><td rowspan="2"></td></tr>
<tr><td>11</td></tr>
</table>

(b) The Conventional scheme

<table>
<tr><th>PRB</th><th>Cell1</th><th>Cell2</th><th>Cell3</th></tr>
<tr><td>0</td><td rowspan="3">$W_{1,ICU}$</td><td rowspan="3">$S_{2\rightarrow1,CEU}$</td><td rowspan="3">$S_{3\rightarrow1,CEU}$</td></tr>
<tr><td>1</td></tr>
<tr><td>2</td></tr>
<tr><td>3</td><td rowspan="3">$S_{1\rightarrow2,CEU}$</td><td rowspan="3">$W_{2,ICU}$</td><td rowspan="3">$S_{3\rightarrow2,CEU}$</td></tr>
<tr><td>4</td></tr>
<tr><td>5</td></tr>
<tr><td>6</td><td rowspan="3">$S_{1\rightarrow3,CEU}$</td><td rowspan="3">$S_{2\rightarrow3,CEU}$</td><td rowspan="3">$W_{3,ICU}$</td></tr>
<tr><td>7</td></tr>
<tr><td>8</td></tr>
<tr><td>9</td><td rowspan="3">IC</td><td rowspan="3">IC</td><td rowspan="3">IC</td></tr>
<tr><td>10</td></tr>
<tr><td>11</td></tr>
</table>

$$PWR\_r = \frac{TxPwrLow}{TxPwrHigh}, \tag{14}$$

and *No ICIC* and *[Pro]* mean that no ICIC scheme was used and the proposed ICIC scheme was applied, respectively. This figure confirms that the proposed ICIC scheme can easily control the user geometry of each cell by adjusting *Thr1* and can considerably improve the CDF of user geometry compared with *No ICIC*. However, an improvement in geometry does not guarantee an improvement in capacity, because bandwidths for individual user are different. Therefore, we should observe a change in capacity according to *Thr1*.

Figure 6 shows capacity performance according to Thr_1, where *AvgCapa* and *5%Capa* indicate the average cell capacity and the 5% cell edge capacity, respectively. In this figure, we see that the 5% cell edge capacity has a maximum value at −55 dBm and rapidly decreases

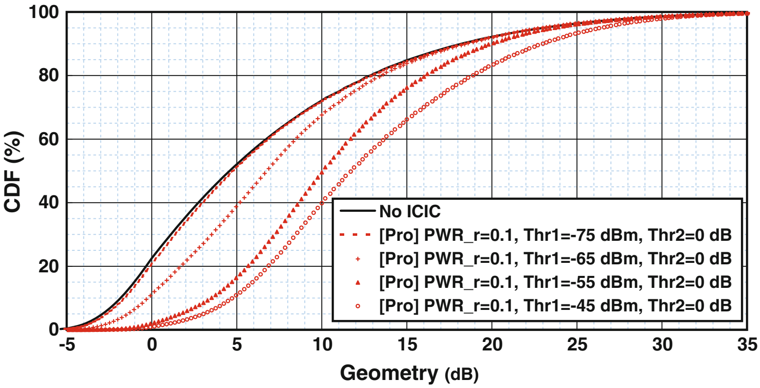

Fig. 5 CDF of geometry obtained using the proposed ICIC scheme for various *Thr1*

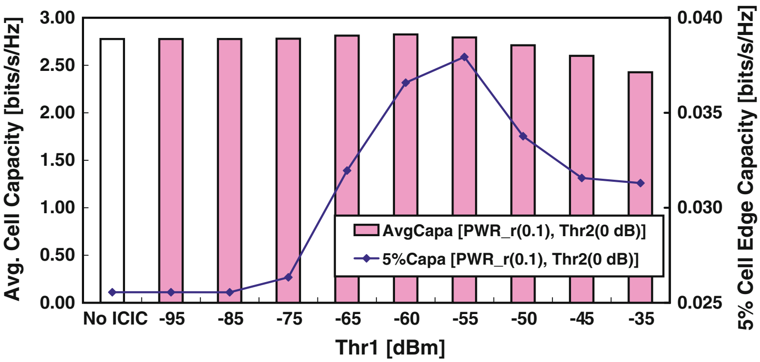

Fig. 6 Capacity obtained using the proposed ICIC scheme for various *Thr1*

as *Thr1* decreases. If *Thr1* is very low, the proposed algorithm judges that many users are in the inner region of the cell (although that is the wrong decision) and thus assigns the whole bandwidth to them. As a result, interference in the cell-edge region increases. Average cell capacity gradually decreases when *Thr1* is higher than −55 dBm because the proposed algorithm judges that many users are in the cell-edge region and thus assigns some of the bandwidth to them.

Next, we observed the effect of *PWR_r*. Figure 7 shows the CDF of geometry according to *PWR_r* when the proposed ICIC scheme uses $Thr1 = 55$ dBm and $Thr2 = 0$ dB. We can also see from this figure that the proposed ICIC scheme can control the user geometry of each cell by adjusting *PWR_r* and can dramatically improve the CDF of user geometry compared with *No ICIC*. As we have mentioned, good geometry does not always mean good capacity.

Figure 8 shows capacity performance according to the value of $Thr2$. In this figure, we can see that the change in 5% cell edge capacity according to $Thr2$ is not as drastic as in the case of *Thr1* because $Thr2$ defines only whether there is one source of strong interference on CEUs or two. If $Thr2$ increases, the proposed algorithm judges that many CEUs are in the region interfered with by two cells, and therefore assigns a relatively small bandwidth to them. As a result, both average cell capacity and 5% cell edge capacity decrease.

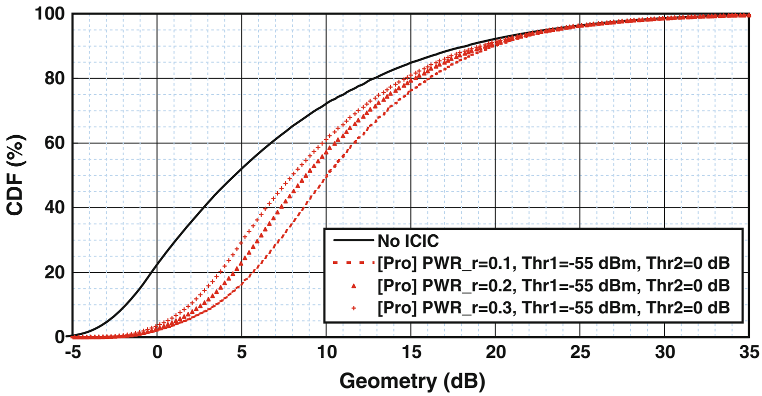

Fig. 7 CDF of geometry obtained using the proposed ICIC scheme for various *PWR_r*

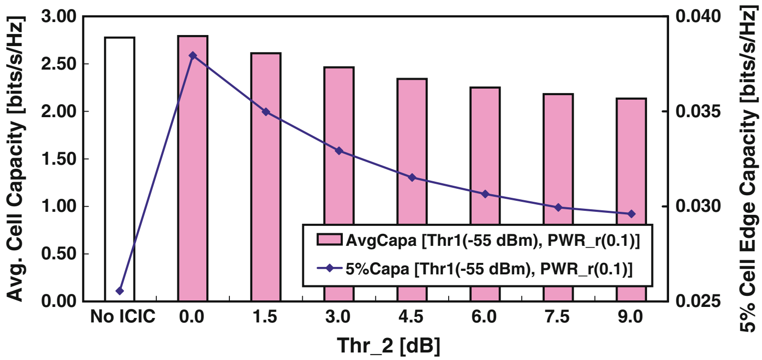

Fig. 8 Capacity obtained using the proposed ICIC scheme for various *Thr2*

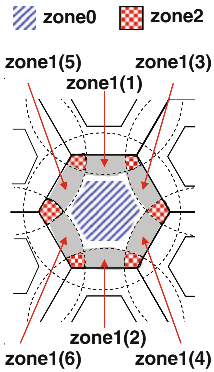

Thr1	zone0	zone1(1)	zone1(2)	zone1(3)	zone1(4)	zone1(5)	zone1(6)	zone2
-75 dBm	0.98198	0.00312	0.00308	0.00318	0.00318	0.0031	0.00236	0
-65 dBm	0.78026	0.03644	0.03566	0.0388	0.03642	0.0362	0.03622	0
-55 dBm	0.36066	0.10686	0.107	0.10788	0.10578	0.10596	0.10586	0
-45 dBm	0.10394	0.15098	0.14832	0.15154	0.1476	0.1489	0.14872	0

(a) PWR_r=0.1, Thr2=0 dB

Thr2	zone0	zone1(1)	zone1(2)	zone1(3)	zone1(4)	zone1(5)	zone1(6)	zone2
0 dB	0.36066	0.10686	0.107	0.10788	0.10578	0.10596	0.10586	0
1.5 dB	0.36066	0.0801	0.07994	0.08082	0.07932	0.08022	0.07818	0.16076
3 dB	0.36066	0.05812	0.05774	0.05972	0.05828	0.0588	0.0571	0.28958
4.5 dB	0.36066	0.04102	0.04044	0.04166	0.04036	0.04096	0.03968	0.39522

(b) PWR_r=0.1, Thr1=-65 dBm

Fig. 9 Zone distributions according to various values of the parameters

On the other hand, Fig. 9 shows changes in zone distributions according to parameters that can be adjusted in the proposed ICIC algorithm.

Figures 10 and 11 show performance comparisons between the proposed scheme and the conventional scheme for geometry and capacity, where *[Conv]* indicates the conventional

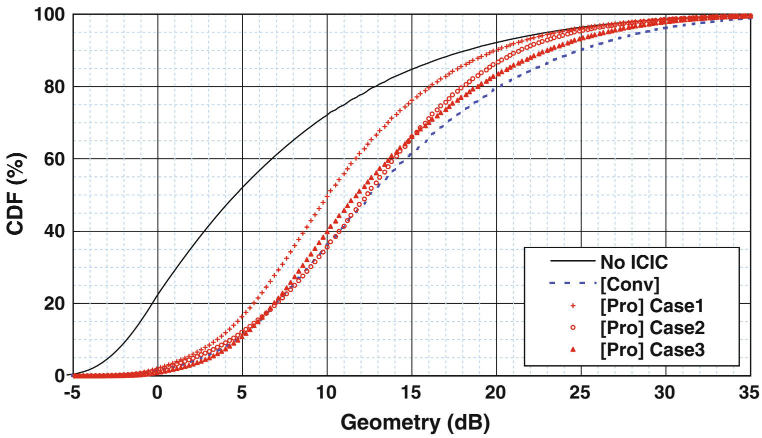

Fig. 10 Performance comparison between the proposed scheme and the conventional schemes in terms of geometry

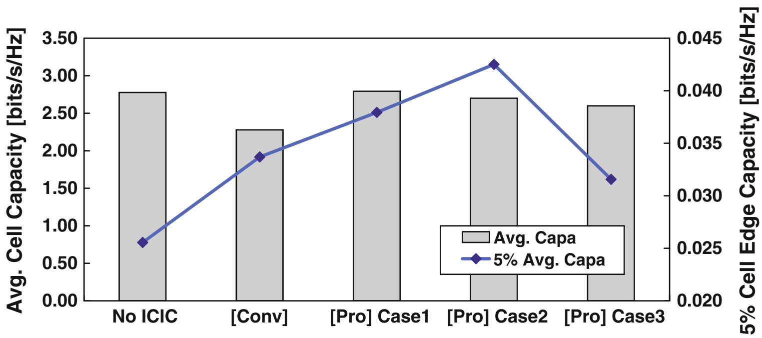

Fig. 11 Performance comparison between the proposed scheme and the conventional schemes in terms of capacity

scheme using $PWR\_r = 0.1$ and the resource allocation given in Table 4. The proposed scheme employs three kinds of parameter sets, *Case1*, *Case2*, and *Case3*, defined as ($PWR\_r = 0.1$, $Thr1 = -55$ dBm, $Thr2 = 0$ dB), ($PWR\_r = 0.01$, $Thr1 = -55$ dBm, $Thr2 = 0$ dB), and ($PWR\_r = 0.1$, $Thr1 = -45$ dBm, $Thr2 = 0$ dB), respectively. We can see from these figures that the proposed scheme can provide meaningful improvement over the conventional system in terms of both the average cell capacity and the 5% cell edge capacity, through efficient resource allocation and threshold-based region decisions.

Note that the presented performances are just examples of various possible implementations of the proposed algorithm and have not been optimized. We also note that the performance of the conventional scheme is not optimum, although it is the best result obtained from many simulations.

Finally, we conclude that the proposed ICIC scheme can improve the 5% cell edge capacity while keeping a similar average cell capacity compared with *No ICIC*.

5 Conclusions

In this paper, we proposed an intercell interference coordination scheme for OFDM-based 4G cellular systems. In this scheme, each cell is divided into several regions based on threshold values, and frequency resources are partially or wholly allocated to each region with a different maximum TX power according to the interference environment.

The performance of the proposed scheme has been evaluated through multi-cell system-level simulations. Simulation results have verified that the proposed scheme improves on conventional systems in terms of outage probability on cell edges and of the average cell throughput.

Because the proposed scheme uses only a few parameters (i.e., threshold and power ratio) and the existing measurements of conventional systems, it can be implemented with low complexity and can be a practical solution for interference mitigation. In addition, we can easily control the trade-off between the average cell capacity and the 5% cell edge capacity by adjusting the parameters. Therefore, the proposed scheme has a high degree of flexibility. Finally, the principles of the proposed scheme can be readily applied to other zone-based interference mitigation schemes.

References

1. 3GPP. (2006). Requirement for evolved UTRA (E-UTRA) and evolved UTRAN (E-UTRAN), *TR 25.913*.
2. CEWiT. (2008). IMT advanced technical requirements—an India perspective, *3GPP REV-080050*, Shenzhen, China, April 7–8.
3. 3GPP. (2008). Requirement for further advancements for E-UTRA (LTE-Advanced), *TR 36.913*.
4. Ericsson. (2005). Inter-cell interference handling for E-UTRA, *3GPP R1-050764*, London, UK, Aug. 29–Sep. 2.
5. RITT. (2005). Inter-cell interference mitigation based on IDMA, *3GPP R1-050608*, Sophia Antipolis, France, June 20–21.
6. Qualcomm. (2005). Description and simulation of interference management technique for OFDMA based E-UTRA downlink evaluation, *3GPP R1-050896*, London, United Kingdom, Aug. 29–Sep. 2.
7. Qualcomm. (2005). Further description of dynamic FFR for OFDM based E-UTRA downlink, *3GPP R1-051123*, San Diego, USA, Oct. 10–14.
8. Alcatel. (2005). Interference coordination in new OFDM DL air interface, *3GPP R1-050407*, Athens, Greece, May 9–13.
9. Alcatel. (2005). Multi-cell simulation results for interference coordination in new OFDM DL, *3GPP R1-050694*, London, United Kingdom, Aug. 29–Sep. 2.
10. Alcatel. (2005). Interference coordination for evolved UTRA uplink access, *3GPP R1-050695*, London, United Kingdom, Aug. 29–Sep. 2.
11. ETRI. (2005). Inter-cell interference management in practical environments, *3GPP R1-050808*, London, UK, Aug. 29–Sep. 2.
12. ETRI. (2005). Resource allocation for interference mitigation with symbol repetition in E-UTRA downlink, *3GPP R1-051085*, San Diego, USA, Oct. 10–14.
13. Kwon, J., Lee, H., & Ahn, J. (2008). Perofrmance of unified inter-cell interference avoidance and cancellation in OFDM mobile cellular systems. *The Journal of Korea Informtion and Communications Society, 33*(4), 371–376.
14. Huawei. (2005). Soft frequency reuse scheme for UTRAN LTE, *3GPP R1-050507*, Athens, Greece, May 9–13.
15. Huawei. (2005). Further analysis of soft frequency reuse Scheme, *3GPP R1-050841*, London, United Kingdom, Aug. 29–Sep. 2.
16. Ericsson & NTT DoCoMo. (2006). Downlink and uplink inter-cell interference co-ordination/avoidance impact on the specifications, *3GPP R1-060586*, Denver, USA, Feb. 13–17.
17. Siemens. (2005). Interference mitigation—considerations and results on frequency reuse, *3GPP R1-050738*, London, United Kingdom, Aug. 29–Sep. 2.
18. Siemens. (2006). Interference mitigation by partial frequency Reuse, *3GPP R1-060670*, Denver, USA, Feb. 13–17.
19. LGE. (2005). Interference mitigation in evolved UTRA/UTRAN, *3GPP R1-050833*, London, United Kingdom, Aug. 29–Sep. 2.

20. Nokia. (2005). UL interference control considerations, *3GPP R1-050813*, London, United Kingdom, Aug. 29–Sep. 2.
21. LGE. (2005). Standard aspects of interference coordination for E-UTRA, *3GPP R1-051051*, San Diego, USA, Oct. 10–14.
22. NEC. (2008). NECs view on requirements of LTE advanced, *REV-080021, 3GPP RAN IMT Advanced Workshop*, Shenzhen, China, April 7–8.
23. Alcatel-Lucent. (2008). Requirements and concepts for LTE advanced, *REV-080044, 3GPP RAN IMT advanced workshop*, Shenzhen, China, April 7–8.
24. Motorola. (2008). LTE advanced technical proposals, *REV-080011, 3GPP RAN IMT advanced workshop*, Shenzhen, China, April 7–8.
25. Ericsson. (2008). LTE-Advanced, technology components, *REV-080030, 3GPP RAN IMT advanced workshop*, Shenzhen, China, April 7–8.
26. Alcatel-Lucent. (2008). LTE-advanced candidate technologies, *REV-080048, 3GPP RAN IMT advanced workshop*, Shenzhen, China, April 7–8.
27. 3GPP TSG RAN. (2010). *Evolved universal terrestrial radio access (E-UTRA); physical channels and modulation*, TS 36.211 (Release9), March 2010.
28. Ericsson. (2008). Additional RSRP reporting trigger for ICIC, 3GPP R1-081536, Shenzhen, China, March 31–April 4.
29. 3GPP TSG RAN. (2010). *Evolved universal terrestrial radio access (E-UTRA); physical layer procedures*, TS 36.213 (Release9), Sep. 2010.
30. 3GPP TSG RAN. (2006). Physical layer aspects for evolved Universal terrestrial radio access (UTRA), *3GPP TR 25.814*.

Author Biographies

Cheolwoo You received the B.S., M.S., and Ph.D. degrees in electronics engineering from Yonsei University, Seoul, Korea, in 1993, 1995, and 1999, respectively. From Jan. 1999 to April 2003, he worked as a Senior Research Engineer with the LG Electronics, Gyeonggi, Korea. During 2003–2004, he was a Senior Research Engineer at the EoNex, Songnam, Korea. From August 2004 to July 2006, he was with the Samsung Electronics, Suwon, Korea. Since September 2006, he has been with the Department of Information and Communications Engineering, Myongji University, Gyeonggi, Korea. His research areas are BS/MS modem design, communication theory, signal processing, and advanced channel codes for mobile/nomadic communication systems. He is currently interested in new Multiple Access schemes, Adaptive Resource Allocation, AMC, MIMO systems, advanced FEC, and Relay schemes for 4G communication systems.

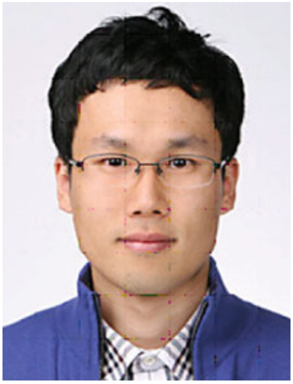

Gilsang Yoon received the B.S. degree in Electronics and Computer Engineering from Chonnam National University, Gwangju, Korea in 2008. He is currently in Chonnam National University, Gwangju, Korea from 2008 as a master student in the School of Electronics & Computer Engineering. His research interests include mobile and wireless communication systems.

Changwoo Seo received the B.S. degree in Information and Communication Engineering from Sangmyung University, Cheonan, Korea in 2009. He is currently in Chonnam National University, Gwangju, Korea from 2009 as a master student in the School of Electronics & Computer Engineering. His research interests include MIMO and OFDM systems.

Sherlie Portugal received the B.S. in Electronic and Telecommunication Engineering from the Technological University of Panama, Panama, in 2006. From 2007 she was worked for the School of Electrical Engineering of the Technological University of Panama and, is currently a master student in the School of Electronics & Computer Engineering of Chonnam National University, South Korea. Her research fields include: MIMO, OFDM, Coding Decoding Algorithms for STC and Multiplexing Schemes and General Wireless Communications.

Gihwan Park received the B.S. degree in Electronics and Computer Engineering from Chonnam National University, Gwangju, Korea in 2011. He is currently in Chonnam National University, Gwangju, Korea from 2011 as a master student in the School of Electronics & Computer Engineering. His research interests include mobile and wireless communication systems.

Taejin Jung received the B.S., M.S., and Ph.D. degrees in electronic and electrical engineering from Pohang University of Science and Technology (POSTECH), Pohang, Korea, in 1996, 1998, and 2003, respectively. In 2003, he was with ETRI, Korea, as a Senior Research Staff Member and worked on the development of efficient receiving algorithms for High Division TV (HDTV). In 2004, he joined the school of electronics and computer engineering, Chonnam National University (CNU), Korea. His research interests are efficient encoding/decoding algorithms for STC, MIMO and MIMO-OFDM, and modem designs for broadband wireless communication systems.

Huaping Liu received his B.S. and M.S. degrees from Nanjing University of Posts and Telecommunications, Nanjing, P. R. China, in 1987 and 1990, respectively, and his Ph.D. degree from New Jersey Institute of Technology, Newark, NJ, in 1997, all in electrical engineering. From July 1997 to August 2001 he was with Lucent Technologies, New Jersey. In September 2001, he joined the School of Electrical and Computer Engineering at Oregon State University, where he has been an associate professor since June 2006. He currently serves as an Associate Editor for the IEEE Transactions on Vehicular Technology and IEEE Communications Letters.

Intae Hwang received the B.S. degree in Electronics Engineering from Chonnam National University, Gwangju, Korea in 1990 and the M.S. degree in Electronics Engineering from Yonsei University, Seoul, Korea in 1992, respectively and the Ph.D. degree in Electrical & Electronics Engineering from Yonsei University, Seoul, Korea in 2004. He had been as a senior engineer at LG Electronics from 1992 to 2005. He is currently in Chonnam National University, Gwangju, Korea from 2006 as a Professor in the School of Electronics & Computer Engineering. His current research activities are in digital & wireless communication systems, mobile terminal system for next generation, physical layer software for mobile terminal, efficient algorithms for AMC, MIMO, MIMO-OFDM and ICIM, and Relaying scheme for wireless communication.